Structure of vapour deposited adenine on a nanostructured perovskite surface studied by STM

Donald G. Fraser,*[a] David S. Deak,[b] Shasha Liu[a] and Martin R. Castell[b]

Received 21st December 2005, Accepted 3rd January 2006
First published as an Advance Article on the web 10th July 2006
DOI: 10.1039/b518079a

The structures of vapour deposited layers of adenine on a nanostructured $SrTiO_3$(001) surface have been investigated by scanning tunneling microscopy (STM). The STM images reveal details of self-organization of adenine monolayers in which adsorption is controlled both by substrate nanostructure and by intermolecular H-bonding of adenine molecules. Detailed examination of STM images suggests that at least three different ordering structures are possible and two distinct orientations may exist with opposite chirality.

Introduction

The origin of biological homochirality is a key question for research on the origin of life. Chiral selectivity is also important in the purification of pharmaceuticals and in the development of biosensors. In contact with aqueous solution, selective surface reactions of chiral molecules with particular crystal faces have been observed in a small number of naturally occurring minerals.[1] However, there is increasing interest in the self organization of adsorbed molecular layers to form chiral domains and other structures. These can form during deposition from the vapour. Here we report structures observed from the deposition under high vacuum of the nucleic acid base, adenine, on the surface of the perovskite mineral $SrTiO_3$ that condenses with $CaTiO_3$ to form a solid in the earliest stages of planetary formation.[2] The free adenine molecule is planar with a single mirror plane that gives rise to the point group C_s. However adsorption onto a surface breaks this symmetry and adenine behaves as a protochiral molecule and adsorbed adenine is thus chiral.

Infra-red emission from interstellar dust particles has been studied by the ESA space telescope infra-red space observatory (ISO) and observations of the circumstellar disks of Vega-type stars have revealed that the dust shells around these stars contain crystalline silicates.[3,4] Detailed studies of the spectra of the comet Hale–Bopp show that the spectra contain bands most similar to Mg-rich olivine Mg_2SiO_4 rather than pyroxenes ($MgSiO_3$).[5] Moreover the similarity of these spectra with spectra of circumstellar dust shells establishes a possible link between the primordial solar system dust preserved in comets and the dust around young stars.

Reactions on the surfaces of interstellar dust grains are probably a major source of complex organic material in space. This material includes simple molecules such as CH_4, NH_3 and HCN as well as diamonds, aldehydes, ketones, acids, aromatic hydrocarbons and possibly fullerenes and bucky tubes.[6,7] Although the initial reported explicit spectroscopic identification of glycine[8] in hot molecular cores associated with early phases of star formation is probably erroneous, its likely presence in these regions is not in dispute and may be of central importance to studies of the origin of life in the universe.[9] These direct observations in space are supported by studies of the organic contents of primitive meteorites. The carbonaceous chondrite meteorite Murchison, for example, that was recovered shortly after falling in 1969, not only contains a very large number of amino acids, but most have no natural terrestrial occurrence and recent studies have shown only a slight enantiomeric excess of L-isomers.[10,11]

[a] *Department of Earth Sciences, University of Oxford, Parks Road, Oxford, UK OX1 3PR*
[b] *Department of Materials, University of Oxford, Parks Road, Oxford, UK OX1 3PH*

Mg-rich olivines such as those present in interstellar dust are, together with pyroxenes, also major constituents of basalts which cover some 70% of the Earth's surface. At high pressure, olivine breaks down to form $MgSiO_3$ perovskite. This is probably the most abundant mineral on Earth and occurs stably throughout the lower mantle. Mg perovskites of this type have been identified in shock-induced high pressure veins in meteorites.[12] Recently, Sr-containing $CaTiO_3$ perovskites have been identified, again in the meteorite Murchison, but in contrast, are primary vapour condensates from the early solar system gas cloud preserved as inclusions in the meteorite.[2]

The Sr-bearing perovskite $SrTiO_3$ has also attracted substantial interest as a material for novel electronic systems[13,14,17] and can form a rich variety of surface nanostructures.[15–17] The surface of $SrTiO_3(001)$ is well-studied[22–27] and therefore provides an exciting oxide substrate for investigating heterogeneous catalysis and surface organization of molecules such as adenine. $SrTiO_3$ also exhibits interesting photocatalytic properties[18] which may offer further possibilities in exploring the ways in which biomolecules behave in a photo-active environment. Recent laboratory data[19] show that adenine is stable in simulated space conditions at 12 K under UV irradiation.

In previous work we have presented detailed *ab initio* calculations of the interaction of water molecules with the nominal MgO(100) surface, together with AFM images of the resulting etch pits.[20] This combined theoretical and observational work showed that (hk0) and (111) step edges on the surface play a determining role in the overall interaction of H_2O molecules with nominal (100) MgO surfaces. Here we extend this paradigm to investigate the role of surface nanostructures in controlling the orientation and organization of adsorbed prebiotic molecules. We report the results of an atomic resolution STM study, under UHV conditions, of the organization of adenine molecules and layers on $SrTiO_3$ surface nanostructures.

Experimental

Single crystals of Nb-doped (0.5% weight) $SrTiO_3$ with epi-polished surfaces were supplied by PI-KEM UK Ltd., as described previously.[15] (Samples of 1.0% La-doped $SrTiO_3(001)$ were also previously used, and produced similar results to what is described here.) These samples were introduced into an ultrahigh vacuum (UHV) chamber (10^{-8} Pa) of a STM system (JEOL JSTM4500S) and were degassed through thermal annealing up to 800 °C for several hours. Annealing was achieved by resistive heating of the semiconducting samples and temperature measurements were performed through a viewport of the UHV chamber using an optical pyrometer. The nanostructured surfaces were prepared by argon ion (Ar^+) sputtering followed by a 30 min UHV anneal of the $SrTiO_3(001)$ samples at 960 °C. Ar^+ sputtering was achieved using a VG Microtech Ion Gun System EX03 which operates at an Ar gas pressure maintained at $\sim 4.5 \times 10^{-4}$ Pa. The ion beam energy was 0.5 keV and the beam-sample current was kept at around 5 μA for 7–15 min. By controlling the time, temperature, and number of anneals, it is possible to form particular types of nanostructures and their respective 2D domains on the (001) surface.

The nanostructured surfaces were imaged in constant current mode using chemically etched tungsten tips in the STM system. Adenine adsorption was achieved by introducing adenine powder (Sigma Aldrich >99%) into a PBN (pyrolytic boron nitride) Knudsen cell within the STM UHV system. The cell was degassed thoroughly for 3 days at around 100 °C and then heated to 190 °C to allow the adenine to evaporate. Previous work indicates that adenine sublimes without thermal decomposition at this temperature with a vapour pressure of around 100 Pa[21] and molecular beams of adenine were allowed to impinge on the $SrTiO_3$ surface for a few minutes for each run.

Results

A clean nanostructured surface of $SrTiO_3(001)$ is illustrated in the STM image of Fig. 1. As shown in Fig. 1a, the nanostructures are highly ordered lines oriented in the ⟨100⟩ crystallographic directions which cover the entire surface. There are several types of nanostructures that form on $SrTiO_3(001)$ surfaces.[17] Three prevalent types of linear nanostructures, or nanolines, are shown in detail in the STM image of Fig. 1b. These nanolines align next to each other in a close-packed manner. A surface region that hosts more than one nanostructure of the same type in the close-packed manner is a *domain*.

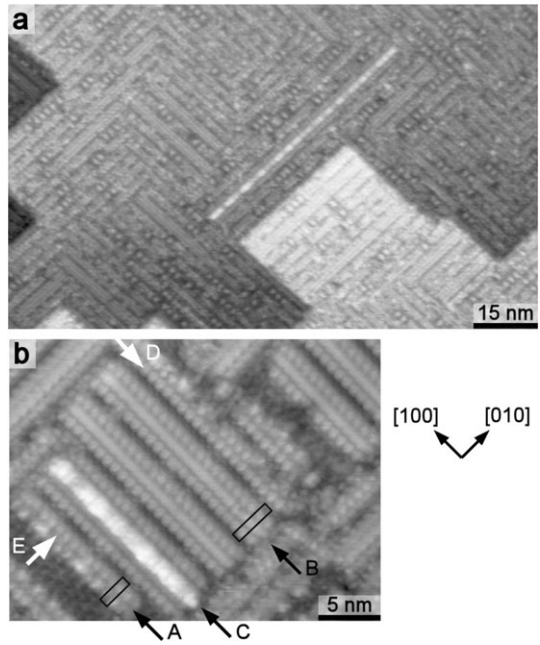

Fig. 1 (a) An STM image of the nanostructured $SrTiO_3(001)$ surface which is used as a template for depositing adenine molecules. (b) A high-resolution STM image showing a surface structure of dilines, trilines, and tetralines pointed out by arrows A, B, and C, respectively. The rectangle covering the diline indicates a (6×2) surface pattern, whereas the rectangle on the triline exhibits a (9×2) surface structure. Imaging parameters: (a), [123.2×75.7 nm^2; $V_s = 1.5$ V; $I_t = 0.10$ nA]. (b), [29.9×22.8 nm^2; $V_s = 1.8$ V; $I_t = 0.23$ nA].

One type of nanoline is pointed out by arrow A in Fig. 1b. Its structure consists of two protruding rows of atomic complexes, and is hence termed a *diline*. Dilines have a width of around 2.4 nm (6 unit cells of $SrTiO_3$), and exhibit a 0.8 nm (2 unit cells) periodicity along the length of a diline. A (6×2) surface pattern, indicated on the diline in Fig. 1b by the rectangle, is formed when dilines are arranged in close-packed domains. Arrow B in Fig. 1b points to a similar kind of nanostructure which is wider and hosts a seemingly continuous backbone between the rows of atomic complexes. This three-rowed structure is termed a *triline*. Trilines occupy a 3.1 nm (9 unit cells) width and maintain the same 0.8 nm lengthwise periodicity as the dilines. Hence a (9×2) surface pattern emerges, as indicated by the rectangle drawn on the triline of Fig. 1b. The third nanoline structure is pointed out by arrow C in Fig. 1b, which is double the width of a diline and is termed a *tetraline*. The backbone on a tetraline is brighter, and hence wider and more elevated than the backbones of trilines. Auger electron spectroscopy (AES) performed on these surfaces shows that the nanostructured surfaces are rich in TiO_2 compared to a (001) sample cleaved in UHV.

STM of sub-monolayer deposition of adenine on this nanostructured surface showed poorly resolved and indistinct islets of adsorbed material. However, on further vapour deposition and annealing, a monolayer of adsorbed adenine was formed which was highly ordered on these $SrTiO_3$ nanostructures as is shown in Fig. 2. We determine the sample coverage through analysis of our STM images, and a monolayer corresponds to the amount that produces saturation coverage. Three types of substrate control can be observed in differently ordered adenine domains.

On (6×2)-patterned diline domains, adenine forms rows with a 2.4 nm (6 unit cell) width periodicity, identical to that observed for clean $SrTiO_3$ diline nanostructures. However, careful examination of Fig. 2 also shows a periodicity at high resolution running along the length of the dilines. This is shown in detail in Fig. 2c and a height profile is shown by the black curve F in Fig. 2e. The structural periodicity imposed on the diline and shown in Fig. 2e has a repeat distance of around 1.6 nm (black curve F). In contrast, along-length periodicity of the clean substrate in Fig. 1 is also shown in Fig. 2e (grey curve D) and has a periodicity of 0.8 nm.

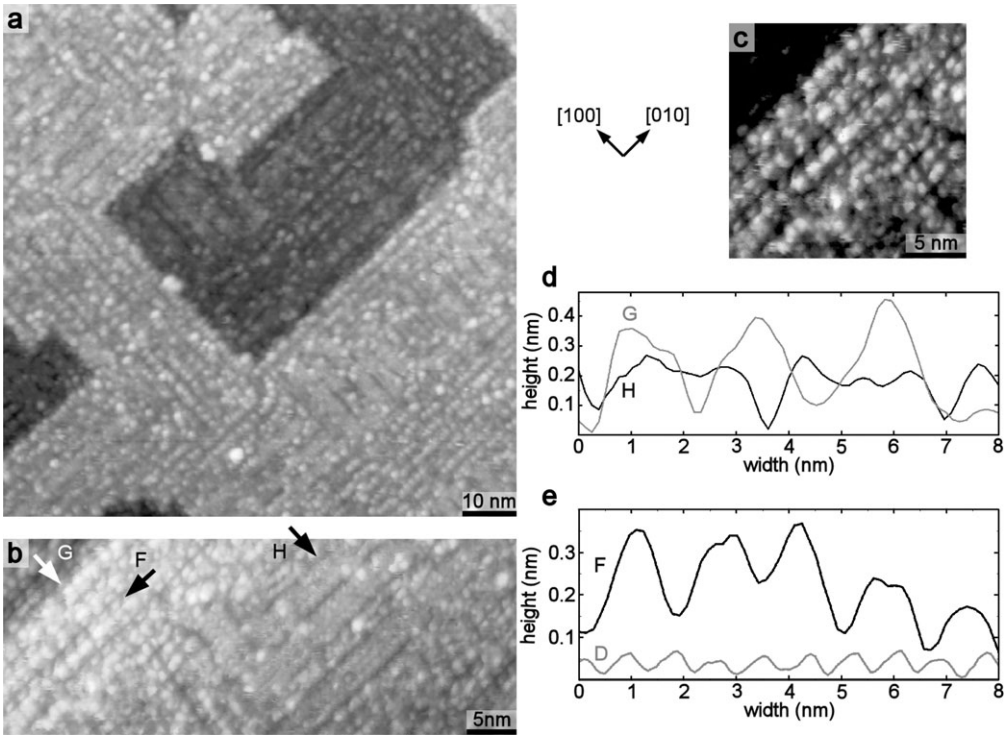

Fig. 2 STM images: (a) of a monolayer of adenine assembled on diline and triline domains, (b) illustrating structural features of the adenine ordering, (c) is a high-contrast STM image exemplifying details of the surface ordering shown in (b). (d) The grey and black profiles are relative heights and are drawn from where the arrows G and H point in image (b), respectively. The black profile in (e) is drawn from where arrow F points in image (b), whereas the grey profile in (e) is taken from where arrow D points on the clean surface in the previous Fig. 1(b). Imaging parameters: (a) [95×95 nm^2; $V_s = 1.8$ V; $I_t = 0.04$ nA]. (b) [51.4×19.7 nm^2; $V_s = 1.8$ V; $I_t = 0.05$ nA]. (c) [19.6×19.6 nm^2; $V_s = 1.8$ V; $I_t = 0.05$ nA].

Adsorption on triline nanostructures is also illustrated in Fig. 2b, in the region indicated by arrow H. As with diline adsorbates, this also preserves the same 9-unit cell width periodicity of the triline substrate. A height profile across a triline domain covered in adsorbate is shown in Fig. 2d (black curve H). This shows that the adenine structures on trilines are at least 0.1 nm lower than those on dilines, suggesting that more than one configuration of adenine molecules is possible on these nanostructured surfaces.

This effect is still more pronounced on tetraline features as shown in Fig. 3. Tetraline backbones rise 0.1 nm above the heights of dilines and trilines, as demonstrated by the grey profile E in Fig. 3b. However, adenine molecules bound to tetraline sites yield a profile $\sim$0.5 nm above the surrounding adenine molecules (profile J in Fig. 3b) thus giving rise to adenine adsorbate structures that either (i) order with elevated features on tetralines, 0.4 nm above the thickness of adenine on dilines and trilines, (ii) exhibit a high local density of electronic states over the tetraline backbone, or (iii) a combination of the two.

Discussion

At low coverage, adsorbed adenine on nanostructured $SrTiO_3(001)$ forms apparently random and ill-formed islets. However, on forming a monolayer, surface assembled adenine on these $SrTiO_3$ perovskite nanostructures is observed in three forms:

(1) on diline surfaces—rows of adenine with 6 unit cell periodicity. Each row undulates with peaks reaching at least 0.3 nm (grey profile G in Fig. 2d). This contrasts with the 0.2 nm height of dilines themselves.

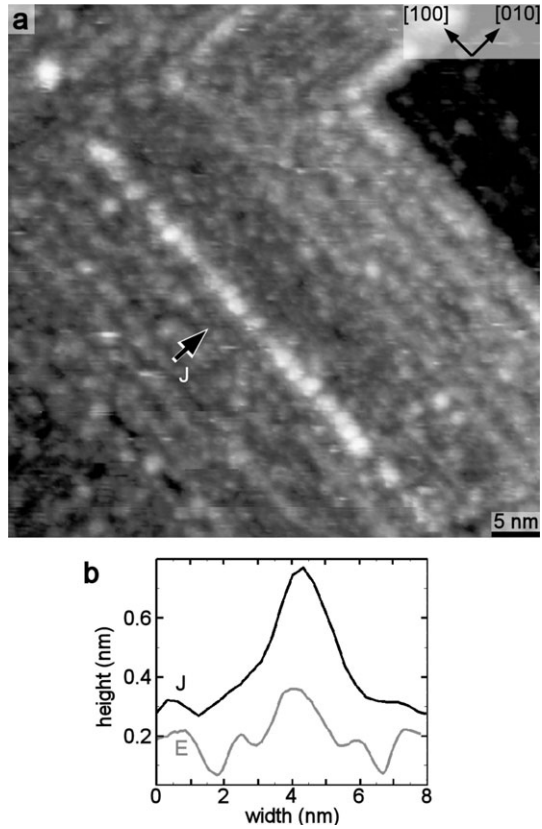

Fig. 3 (a) An STM image illustrating adenine assembly on a tetraline. (b) The black height profile is taken from where the arrow J points in (a), and the grey profile is drawn from arrow E in Fig. 1(b). The heights of the profiles in (b) have been offset with respect to each other. Imaging parameters: [55 × 55 nm^2; V_s = 1.9 V; I_t = 0.10 nA].

(2) on triline surfaces—rows exhibit the underlying 9 unit cell periodicity. Rows are wider and shallower on trilines as compared with dilines. Heights are around 0.2 nm, which is comparable to the heights of the trilines (black profile H in Fig. 2d).

(3) on tetralines—adenine protrudes to a height of around 0.5 nm higher than adenine on the surrounding surface. This contrasts with the typical 0.1 nm height of the tetraline backbone over the heights of the shoulder rows or adjacent triline/diline structures.

In addition, at least along diline structures, periodicity of an ordered adenine layer is observed with a repetition of 1.6 nm that compares with the repeat distance of 0.8 nm of the underlying diline structure. This may also be true of adsorption on the triline structure, but at present the data are indistinct.

The structures of ordered monolayers of adenine on highly conducting substrates including Cu(110),[28] Cu(111),[29,30] MoS_2, and graphite,[31–34] have been reported previously. In addition, indistinct STM images have been reported that may allow differentiation between adenine and thymine and between guanine and cytosine molecules adsorbed on reduced $SrTiO_3$.[36]

Deposition of adenine on Cu(110) results in the formation of molecular one-dimensional chains of adenine dimers[28] while on the Cu(111) surface, STM studies show short range ordering to form one dimensional chains and 2D honeycomb structures.[29,30]

On graphite(0001), different structures of assembled monolayers have been described[31–33] and a combined theoretical, LEED and STM study has shown that the observed molecular structure is commensurate with the graphite substrate, forming a hydrogen-bonded network with four bonds per molecule.[34] In this study, the contrast in the STM image was interpreted as being dominated by geometrical height variations of the tilted molecules. A recent *ab initio* calculation[35] of the energies of

adsorption of adenine on graphite using DFT under GGA showed, in agreement with experiment, that calculation yields a relatively large adsorption energy of about 1 eV. The exchange correlation energy overcompensates the Pauli repulsion forces and hinders adenine mobility on the graphite(0001) surface. These calculations demonstrate that even in cases of chemically inert surfaces, there is a noticeable influence of the substrate on the molecular electronic structure and mobility.

In the present study, the structures shown in Fig. 2 and 3 show pronounced ordering of adenine molecules on nanostructures of the $SrTiO_3$ substrate. This is in accord with the *ab intio* calculations of the energies of adenine adsorption even on the graphite surface[35] in which the energetics of interactions of the surface and the adsorbed adsystem are of comparable magnitude to intermolecular hydrogen bonds. On $SrTiO_3$ interactions between adenine molecules and the perovskite hosted nanostructures seem sufficiently strong to dominate the observed adenine ordering.

The periodicity of the underlying $SrTiO_3$ diline nanostructure is 0.8 nm (see Fig. 1 and 2e) while that of the organized adenine monolayer, also shown in Fig. 2e, is 1.6 nm. A recent detailed STM, LEED, EELS and *ab initio* study of self-assembly of adenine on Cu(110) shows the development of one dimensional chains and chiral domains composed in both cases of ordered adenine dimers in which the double purine rings are linked by hydrogen bonding between pairs of N-atoms.[28] These chain-forming adenine dimers have a periodicity of 0.78 nm and a width of 0.8 nm.

In the present case, deposition and organization on the $SrTiO_3$ substrate may also take place *via* the formation of adenine dimers. However the strong 1.6 nm periodicity observed in Fig. 2b and 2e suggests that organization to form any higher dimensionality such as chains, may require corrugation of the chains so that only every second pair is observed at the maximum height in the STM image.

Detailed examination of the image contrast in Fig. 2b and 2c suggests that there may indeed be further self-organisation along at least the diline nanostrustures with chains of elements being related by a mirror plane approximately perpendicular to the diline and thus facing each other. Investigation of the detail of these structures may prove feasible in the near future. However if true, this self-organization carries the tantalizing prospect of observing chiral self-organization *in situ* on these nanostructured oxide surfaces.

Summary and conclusions

Adenine adsorbs on nanostructured $SrTiO_3(100)$ surfaces to form random islets at low coverage but in monolayers, forms organized arrays on diline, triline and tetraline nanostructures. At least on diline structures, the adenine layer has a periodicity related to the underlying diline structure. Its width mirrors the 6×2 surface pattern, 2.4 nm repeat distance of the diline. However, ordering along the diline structure occurs with a 1.6 nm periodicity in contrast to the 0.8 nm repeat of the underlying 6×2 pattern. We believe that adenine may adsorb on nanostructured $SrTiO_3$ as self-organized chains of $(ad)_2$ dimers with chains linked by H-bonding and corrugated along the length of the $SrTiO_3$ dilines. Height profiles suggest that this may also be true for triline structures. The possibility of self-organisation of adsorbed adenine to form polymeric chiral domains lies at the limit of present resolution.

References

1 R. M. Hazen, T. R. Filley and G. A. Goodfriend, *Proc. Natl. Acad. Sci. 98*, 2001, 5487–5490.
2 S. B. Simon, A. M. Davis, L. Grossman and K. D. McKeegan, *Meteorit. Planet. Sci.*, 2002, **37**, 533–548.
3 C. Waelkens, L. B. F. M. Waters, M. S. de Graauw, E. Huygen, K. Malfait, H. Plets, B. Vandenbussche, D. A. Beintema, D. R. Boxhoorn, H. J. Habing, A. M. Heras, D. J. M. Kester, F. Lahuis, P. W. Morris, P. R. Roelfsema, A. Salama, R. Siebenmorgen, N. R. Trams, N. R. van der Bliek, E. A. Valentijn and P. R. Wesselius, *Astron. Astrophys.*, 1996, **315**, L245.
4 L. B. F. M. Waters, F. J. Molster, T. de Jong, D. A. Beintema, C. Waelkens, A. C. A. Boogert, D. R. Boxhoorn, Th. de Graauw, S. Drapatz, H. Feuchtgruber, R. Genzel, F. P. Helmich, A. M. Heras, R. Huygen, H. Izumiura, K. Justtanont, D. J. M. Kester, D. Kunze, F. Lahuis, H. J. G. L. M. Lamers, K. J. Leech, C. Loup, D. Lutz, P. W. Morris, S. D. Price, P. R. Roelfsema, A. Salama, S. G. Schaeidt, A. G. G. M. Tielens, N. R. Trams, E. A. Valentijn, B. Vandenbussche, M. E. van den Ancker, E. F. van Dishoeck, H. van Winckel, P. R. Wesselius and E. T. Young, *Astron. Astrophys.*, 1996, **315**, L361.
5 J. Crovisier, K. Leech, D. Bockelée-Morvan, T. Y. Brooke, M. S. Hanner, B. Altieri, H. U. Keller and E. Lellouch, *Science*, 1997, **275**, 1904–1907.

6 Y. J. Kuan, S. B. Charnley, H. C. Huang, Z. Kisiel, P. Ehrenfreund, W. L. Tseng and C. H. Yan, *Adv. Space Res.*, 2004, **33**, 31.
7 P. Ehrenfreund and S. B. Charnley, *Annu. Rev. Astron. Astrophys.*, 2000, **38**, 427.
8 Y. J. Kuan, S. B. Charnley, H. C. Huang, W. L. Tseng and Z. Kisiel, *Astrophys. J.*, 2003, **593**, 848.
9 D. G. Fraser, *Life in the Universe*, ed. J. Seckbach *et al.*, Springer, 2004, p. 149.
10 M. H. Engel and B. Nagy, *Nature*, 1982, **837**, 296.
11 J. R. Cronin and S. Pizarello, *Science*, 1997, **275**, 951–955.
12 N. Tomioka and K. Fujino, *Science*, 1997, **277**, 1084–1086.
13 D. W. Reagor and V. Y. Butko, *Nat. Mater.*, 2005, **4**, 593–596.
14 D. Kan, T. Terashima, R. Kanda, A. Masuno, K. Tanaka, S. Chu, H. Kan, A. Ishizumi, Y. Kanemitsu, Y. Shimakawa and M. Takano, *Nat. Mater.*, 2005, **4**, 816–819.
15 (*a*) M. R. Castell, *Surf. Sci.*, 2002, **505**, 1; (*b*) M. R. Castell, *Surf. Sci.*, 2002, **516**, 33.
16 D. S. Deak, F. Silly, D. T. Newell and M. R. Castell, *J. Phys. Chem. B*, 2006, **110**, 9246–9251.
17 D. S. Deak, *Mater. Sci. Technol.*, in preparation.
18 J. Yin, J. Yi and Z. Zou, *Appl. Phys. Lett.*, 2004, **85**, 689.
19 Z. Peeters, R. Ruiterkamp, O. Botta, S. B. Charnley and P. Ehrenfreund, *Astrophys. J.*, 2000, **593**, 129.
20 J. A. Mejias, A. J. Berry, K. Refson and D. G. Fraser, *Chem. Phys. Lett.*, 1999, **314**, 558.
21 D. P. Glavin, M. Schubert and J. L. Bada, *Anal. Chem.*, 2002, **74**, 6408–6412.
22 B. Cord and R. Courths, *Surf. Sci.*, 1985, **162**, 34.
23 H. Tanaka, T. Matsumoto, T. Kawai and S. Kawai, *Jpn. J. Appl. Phys., Part 1*, 1993, **36**, 1405.
24 N. Erdman, K. R. Poeppelmeier, M. Asta, O. Warschkow, D. E. Ellis and L. D. Marks, *Nature*, 2002, **419**, 55.
25 N. Erdman, O. Warschkow, M. Asta, K. R. Poeppelmeier, D. E. Ellis and L. D. Marks, *J. Am. Chem. Soc.*, 2003, **124**, 10050.
26 O. Warschkow, M. Asta, N. Erdman, K. R. Poeppelmeier, D. E. Ellis and L. D. Marks, *Surf. Sci.*, 2004, **573**, 446.
27 K. Johnston, M. R. Castell, A. T. Paxton and M. W. Finnis, *Phys. Rev. B*, 2004, **70**, 85415.
28 Q. Chen, D. J. Frankel and N. V. Richardson, *Langmuir*, 2002, **18**, 3219.
29 M. Furukawa, H. Tanaka, K. Sugiura, Y. Sakata and T. Kawai, *Surf. Sci.*, 2000, **445**, L58.
30 M. Furukawa, H. Tanaka and T. Kawai, *Surf. Sci.*, 2000, **445**, 1.
31 M. J. Allen, M. Balooch, S. Subbiah, R. J. Tench, W. Siekhaus and R. Balhorn, *Scanning Microsc.*, 1991, **5**, 625.
32 N. J. Tao and Z. Shi, *J. Phys. Chem.*, 1994, **98**, 1464.
33 T. Boland and B. D. Ratner, *Langmuir*, 1994, **10**, 3845.
34 J. E. Freund, M. Edelwirth, P. Kröbel and W. M. Heckl, *Phys. Rev. B*, **55**, 5394–5397.
35 F. Ortmann, W. G. Schmidt and F. Bechstedt, *Phys. Rev. Lett.*, 2005, **95**, 186101.
36 H. Tanaka and T. Kawai, *Mater. Sci. Eng.*, 1995, **C3**, 143.